

# Demand-side Response Strategy of Multi-microgrids Based on an Improved Co-evolution Algorithm

Yang Gao<sup>✉</sup>, *Member, IEEE*, and Qian Ai, *Senior Member, IEEE*

**Abstract**—An effective modeling and optimization method, which takes into account source-load-storage coordination, and full-time collaborative optimization within and outside microgrids, is introduced. Considering the operational conditions of various resources and their interactions, an energy management model for microgrids is proposed aiming at maximization of renewable energy utilization and minimization of overall system costs. The model is suitable for both real-time pricing and time-of-use mechanisms. In microgrids, demand response and economic energy storage dispatch are introduced to enhance self-coordination and self-balancing ability among different resources. Depending on whether there is still an imbalance between supply and demand after coordination within a microgrid, trade between it and external microgrids are optimized in a orderly manner by considering different transaction prices and usage rights. Finally, three different schemes are designed, where the Lagrangian multiplier method as well as a co-evolution algorithm are used to solve and analyze different examples, verifying the reliability and validity of the method proposed in this paper.

**Index Terms**—Co-evolution, demand-side response, multi-microgrids, source-load-storage coordination.

## I. INTRODUCTION

**I**N recent years, with the rapid development of smart grids and the Energy Internet, the number of microgrids in the distribution network increased. The power generation and consumption of each microgrid only considers the maximization of its own interests, ignoring the overall economy. However, the traditional single microgrid only transmits power to the distribution network through medium-voltage lines. Due to the geographical distance between the two, large transmission losses often occur. For this reason, the adjacent microgrids are interconnected to form a microgrid cluster system [1]–[3]. A smooth implementation of microgrids rely on the effective coordination and unification of information and communication, power dispatching, and demand response [4]–[6]. As the most basic optimization and dispatch unit of the microgrid, it has attracted widespread attention from both academia and

industry since its first proposal. Reference [7] showed that the microgrid represents an effective strategy towards large-scale grid-connected transmission and comprehensive utilization of renewable energy. In addition, the group provided a model for the joint dispatch and optimization of both the microgrid and electric vehicles for a grid-connected mode. References [8] and [9] proposed that renewable energy and load-fluctuations can be effectively suppressed by using different energy-storage units. Therefore, an energy management and optimization model for the microgrid was established. In [10], considering the role of wind, solar and storage in the management and optimization process of the microgrid, a model was established with the objective of minimizing the system investment and fuel cost and maximizing the utilization rate of renewable energy. The model was solved by the improved particle swarm optimization method. References [11]–[13] provided a modeling and optimization method for household microgrids with high renewable-energy-penetration rates. This was done to facilitate the local consumption of renewable energy, online energy-management of the microgrid, and the early recovery of user capital. Reference [14] introduced a demand-response mechanism into the energy management and optimal scheduling of a microgrid. The group promotes the close interaction between energy producers and consumers via economic stimulus programs to ensure effective system-operations during the process of buying and selling electricity.

Even though there is an energy-management problem in the collaborative optimization for microgrids with a high renewable-energy penetration rate, current studies rarely consider microgrid internal and external collaborative scheduling problems and the interaction order with neighborhood/non-neighborhood microgrids and the public grid [15]. In [16], an optimal operational model of microgrids based on a multi-agent system was proposed. The purpose is to save the total energy cost expressed as the sum of locally observable convex functions. However, the operating cost of every DG in the microgrid is simplified to be a quadratic function, and the operating characteristics of various DGs are not considered. In [17], aiming at the active distribution network with multi-microgrids access, a centralized coordinated optimization model for multi-microgrids at three periods of peak, normal and low valley generation was established, and solved by the particle swarm algorithm. The closed-loop scheduling scheme proposed in [18] adopts a stochastic model predictive control strategy, which can avoid the forecast errors caused by load demand, real-time electricity prices and high-penetration distributed power sources in the open-loop strategy. With the

Manuscript received November 17, 2020; revised April 1, 2021; accepted April 27, 2021. Date of online publication September 10, 2021; date of current version September 15, 2021. This work was supported by the Shanghai Sailing Program (20YF1418800) and outstanding Ph.D. graduate development scholarship of Shanghai Jiao Tong University.

Y. Gao (corresponding author, email: jigyxky@126.com; ORCID: <https://orcid.org/0000-0003-1497-1185>) and Q. Ai are with the Key Laboratory of Control of Power Transmission and Conversion, Shanghai Jiao Tong University, Shanghai 200240, China.

DOI: 10.17775/CSEEJPES.2020.06150

goal of reducing total system cost, a distributed microgrid operation scheduling strategy was proposed in paper [19], and an improved particle swarm optimization method was used to solve the scheduling problem. However, the impact of different types of load and electricity price strategies on the optimal dispatch were not considered.

This paper proposes a modeling and optimization method that considers source, load, storage, and full-time collaborative optimization within and outside the microgrid. The different distributed generators, load, energy storage units in the microgrid and their directly connected external grid is regarded as a dispatchable resource in the optimization stage, and the characteristics of every schedulable resource are fully considered and the interaction relationship between each other is established. The most significant novelties of this paper are:

1) Based on the principle of maximizing the utilization of renewable energy and minimizing the operational cost of the system, a demand response mechanism is introduced to construct an optimal scheduling model suitable for real-time price and time of use price in multiple scenarios.

2) Lagrange multiplier and co-evolution algorithms are combined in order to solve the model. The former is used to transform constrained optimization problems, and the latter is used to solve unconstrained optimization problems.

3) This paper proposes an optimization strategy suitable for internal autonomy and inter network cooperation, in order to establish a transaction mechanism, so that the priority of neighbor/non-neighbor microgrids is higher than that of the public grid.

The rest of the paper is structured as follows: Section II analyzes the system architecture of multi-microgrids in detail. Section III primarily discusses the energy management optimization model of microgrids and its solving strategy. In Section IV, the optimization results of three different schemes are compared. The main findings and conclusions are summarized in Section V.

## II. MULTI-MICROGRIDS MODEL

Each microgrid is composed of renewable energy, distributed power generation, an energy storage device and customer load, connected to the public grid for operations, and connected with other microgrids through energy channels, and can support each other with electrical energy. Each microgrid has an energy management center to regulate and control the operation of the internal unit, which can conduct information exchange and energy exchange with the upper-level grid, or coordinate and assist with neighboring microgrids. More specifically, microgrids can be characterized by the following features [20]–[22]:

1) *Composition*: Microgrids can be divided into production capacity, energy consumption, and hybrid nodes, according to the energy richness after multi-period node interaction. Among them, the production and energy-consumption nodes, respectively, refer to microgrids that only output or input energy to the outside. Hybrid nodes can experience both scenarios.

2) *Operating mode*: Microgrids can enable the direct trading of electricity with the public grid via grid-connected opera-

tions, alternatively, and they can realize self-balance through self-regulation when off-grid.

3) *Scheduling strategy*: In the process of energy optimization management, each micro-grid can regulate and control the operation of the internal unit, and can conduct information exchange and energy exchange with the external public grid, or coordinate and assist with neighboring micro-grids.

As shown in Fig. 1, the public grid and microgrids are different stakeholders and have their own operational goals. It is necessary to conduct an interest game to determine the exchange power of the tie line. There is a certain mutual assistance relationship between each microgrid, which can complement each other according to its needs to a certain extent, thus improving system operating efficiency and economics of its own operations.

In each microgrid, the energy dispatch and optimization center are responsible for the completion of the following tasks: capacity aggregation, energy distribution, and supply/demand balancing. More specifically, the process consists of using the communication network to transmit the following: monitored source and network load, storage forecast, and response information. The transmission is done after the analysis and decision processing of dispatchable instructions had been formulated. In other words, what is used are primarily the production-units that are based on wind, natural gas, and photovoltaics, as well as the critical loads, interruptible loads, and energy-storage units. The demands of energy-consuming units and regulating units are collected separately, while the matching of production with energy demands is realized through the distribution and balance units.

## III. METHODOLOGY

### A. Objective Function

The objective function of energy management of microgrids is to minimize the operational costs in the whole scheduling cycle  $T$  as:

$$C_{\text{total}} = \sum_{t=1}^T (C_{\text{DG}}(t) + C_{\text{load}}(t) + C_{\text{ES}}(t) + C_{\text{grid}}(t)) \quad (1)$$

Among them,  $C_{\text{total}}$  is the total operational cost of the system;  $C_{\text{DG}}(t)$ ,  $C_{\text{load}}(t)$ ,  $C_{\text{ES}}(t)$  and  $C_{\text{grid}}(t)$  are the operational costs of each distributed generator capacity, load demand, energy storage unit and interaction with the external grid in the period  $t$ .

#### 1) Operating Cost for Generation Units

The main distributed generation units in a microgrid include the micro-gas turbine, photovoltaic power, and wind power. The operational cost of the micro-gas turbine is a quadratic function, while the operational cost of wind power and pv power is a quadratic function. They are expressed as follows:

$$C_{\text{DG}}(t) = C_{\text{MT}}(t) + C_{\text{wind}}(t) + C_{\text{pv}}(t) \quad (2)$$

$$C_{\text{MT}}(t) = \sum_{i=1}^N [(\alpha_{\text{MT},i}(P_{\text{MT},i}(t)))^2 + \beta_{\text{MT},i}P_{\text{MT},i}(t) + \gamma_{\text{MT},i}] \quad (3)$$

$$C_{\text{wind}}(t) = \sum_{i=1}^M (\alpha_{\text{wind},i}P_{\text{wind},i}(t) + \beta_{\text{wind},i}) \quad (4)$$

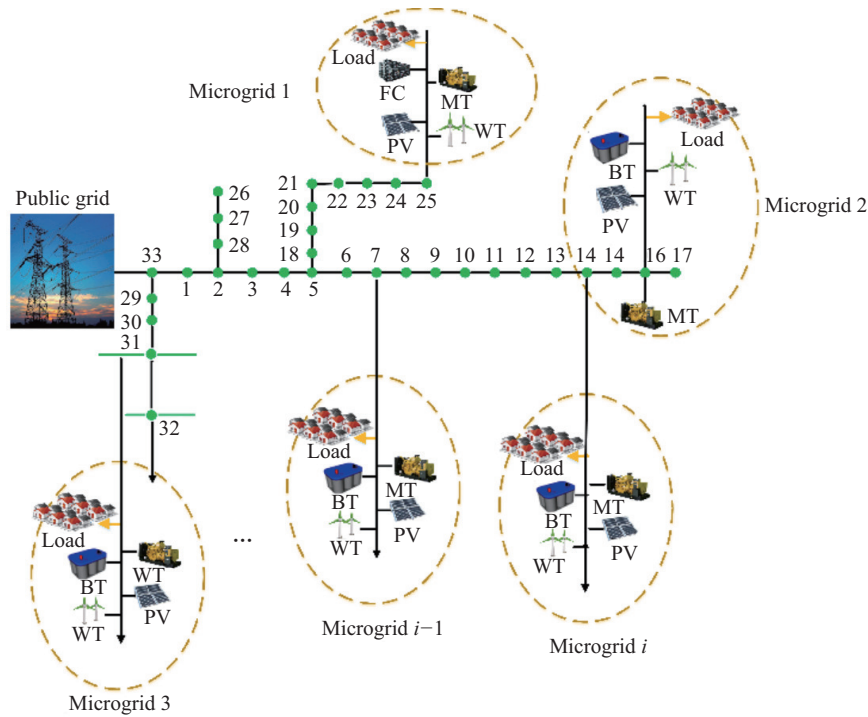


Fig. 1. Framework of multi-microgrids.

$$C_{pv}(t) = \sum_{i=1}^S (\alpha_{pv,i} P_{pv,i}(t) + \beta_{pv,i}) \quad (5)$$

where  $C_{MT}(t)$ ,  $C_{wind}(t)$  and  $C_{pv}(t)$  are the operating cost of the micro-gas turbine, wind power and photovoltaic power unit at period  $t$ , respectively;  $N$ ,  $M$  and  $S$  are the number of various distributed power sources;  $\alpha_{MT,i}$ ,  $\beta_{MT,i}$ ,  $\gamma_{MT,i}$  are the cost coefficients of the micro gas turbine;  $\alpha_{wind,i}$ ,  $\beta_{wind,i}$  are the cost coefficients of wind power;  $\alpha_{pv,i}$ ,  $\beta_{pv,i}$  are the cost coefficients of photovoltaic power.

## 2) Load Demand Cost

The loads in a microgrid are classified into critical load and flexible load according to dispatchable conditions, and their operating costs are determined by the actual load demand and corresponding tariff rates.

$$C_{load}(t) = C_{crit}(t) + C_{flex}(t) \quad (6)$$

$$C_{crit}(t) = - \sum_{i=1}^n [P_{crit,i}(t) \eta_{crit,i}(t)] \quad (7)$$

$$C_{flex}(t) = \sum_{i=1}^m \left[ -P_{flex,i}(t) \cdot (1 - \lambda_{flex,i}(t)) \cdot l_{b\_price}(t) + P_{flex,i}(t) \lambda_{flex,i}(t) \eta_{flex,i}(t) \right] \quad (8)$$

where  $C_{crit}(t)$  and  $C_{flex}(t)$  are the total operating costs of the critical load and the flexible load at time  $t$  respectively;  $n$  and  $m$  are the number of corresponding loads;  $P_{crit,i}(t)$ ,  $P_{flex,i}(t)$  are the critical and flexible load demand at time  $t$ , respectively;  $l_{b\_price}(t)$  is the electricity base price;  $\eta_{crit,i}(t)$ ,  $\eta_{flex,i}(t)$  are the payable rate of the critical load and the compensation rate of the flexible load, respectively.

## 3) Operating Cost of Energy-storage Unit

The operating cost of the energy storage unit primarily includes charging costs, discharge benefits as well as charging/discharging switching costs.

$$C_{ES,i}(T) = \sum_{t=1}^T (C_{char,i}(t) - C_{dis,i}(t)) + C_{switch,i}(T) \quad (9)$$

$$C_{char,i}(t) = P_{char,i}(t) l_{b\_price} \quad (10)$$

$$C_{dis,i}(t) = P_{dis,i}(t) \eta_{dis,i}(t) l_{b\_price}(t) \quad (11)$$

$$C_{switch,i}(T) = (N_{char,i}(T) + N_{dis,i}(T)) \eta_{switch,i}(t) \quad (12)$$

where  $C_{switch,i}(T)$ ,  $N_{char,i}(T)$ ,  $N_{dis,i}(T)$  are the switch state cost, charge to discharge and discharge to charge times at period  $T$ ;  $C_{char,i}(t)$ ,  $C_{dis,i}(t)$  are the charging fee and the discharging income at time  $t$ , respectively;  $\eta_{dis,i}(t)$  is the discharge rate.

## 4) Interaction Costs with External Grid

The cost of interacting with the external grid primarily includes two parts: purchase and sale.

$$C_{grid}(t) = C_{neib}(t) + C_{non\_neib}(t) + C_{public}(t) \quad (13)$$

$$C_{neib}(t) = \sum_{i=1}^p \left[ \left( P_{neib,i}^{buy}(t) \eta_{neib, buy}(t) - P_{neib,i}^{sell}(t) \eta_{neib, sell}(t) \right) \cdot l_{b\_price} \right] \quad (14)$$

$$C_{non\_neib}(t) = \sum_{i=1}^q \left[ \left( P_{non\_neib,i}^{buy}(t) \eta_{non\_neib, buy}(t) - P_{non\_neib,i}^{sell}(t) \eta_{non\_neib, sell}(t) \right) \cdot l_{b\_price} \right] \quad (15)$$

$$C_{\text{public}}(t) = \sum_{i=1}^k \left[ \left( P_{\text{public},i}^{\text{buy}}(t) \eta_{\text{public, buy}}(t) - P_{\text{public},i}^{\text{sell}}(t) \eta_{\text{public, sell}}(t) \right) \cdot l_{\text{b\_price}} \right] \quad (16)$$

where  $C_{\text{grid}}(t)$ ,  $C_{\text{neib}}(t)$ ,  $C_{\text{non\_neib}}(t)$ ,  $C_{\text{public}}(t)$  are the interaction costs between the microgrid and all external direct-connected grids, neighboring/non-neighboring microgrids, and public grids, respectively, at time  $t$ ;  $p$  and  $q$  are the number of neighboring/non-neighboring microgrids respectively.

## B. Constraints

### 1) Capacity-unit Constraints

All DG capacity units need to meet the constraints of unit output power during operations, as follows:

$$P_{\text{DG},i,\min} \leq P_{\text{DG},i}(t) \leq P_{\text{DG},i,\max} \quad (17)$$

$$P_{\text{DG},i}^{\text{actual}}(t) = \begin{cases} \tau_{\text{DG},i}^{\text{high}} P_{\text{DG},i}(t), & \text{if } P_{\text{DG},i}(t) > \mu_{\text{DG},i}^{\text{high}} P_{\text{DG},i}^{\text{rated}}(t) \\ \tau_{\text{DG},i}^{\text{low}} P_{\text{DG},i}(t), & \text{if } P_{\text{DG},i}(t) \leq \mu_{\text{DG},i}^{\text{low}} P_{\text{DG},i}^{\text{rated}}(t) \\ \tau_{\text{DG},i}^{\text{middle}} P_{\text{DG},i}(t), & \text{others} \end{cases} \quad (18)$$

where  $P_{\text{DG}}$  is the type of DG in the microgrid, including the micro-gas turbine, wind power, and photovoltaic power;  $P_{\text{DG},i}^{\text{actual}}(t)$ ,  $P_{\text{DG},i}^{\text{rated}}(t)$  are the actual and rated value of the DG output power, respectively;  $\tau_{\text{DG},i}^{\text{high}}$ ,  $\tau_{\text{DG},i}^{\text{low}}$ ,  $\tau_{\text{DG},i}^{\text{middle}}$  are the conversion coefficient of different levels between actual output power and actual generation power, respectively.

### 2) Constraints of Load Demand

Load demand constraints are determined by the energy consumption and load interruption ratio.

$$P_{\text{crit},i,\min} \leq P_{\text{crit},i}(t) \leq P_{\text{crit},i,\max} \quad (19)$$

$$P_{\text{flex},i,\min} \leq P_{\text{flex},i}(t) \leq P_{\text{flex},i,\max} \quad (20)$$

$$\lambda_{\text{flex},i,\min} \leq \lambda_{\text{flex},i}(t) \leq \lambda_{\text{flex},i,\max} \quad (21)$$

where  $P_{\text{crit},i,\min}$ ,  $P_{\text{crit},i,\max}$ ,  $P_{\text{flex},i,\min}$ ,  $P_{\text{flex},i,\max}$  are the minimum and maximum constraints of critical load and flexible load demand, respectively;  $\lambda_{\text{flex},i,\min}$ ,  $\lambda_{\text{flex},i,\max}$  are the minimum and maximum constraints of the interruptible proportion of the flexible load, respectively.

### 3) Energy-storage Unit Constraints

$$P_{\text{char},i,\min} \leq P_{\text{char},i}(t) \leq P_{\text{char},i,\max} \quad (22)$$

$$P_{\text{dis},i,\min} \leq P_{\text{dis},i}(t) \leq P_{\text{dis},i,\max} \quad (23)$$

$$Q_{\text{ES},\min} \leq Q_{\text{ES},i}(t) \leq Q_{\text{ES},\max} \quad (24)$$

$$Q_{\text{ES},i}(t+1) = Q_{\text{ES},i}(t) + P_{\text{char},i}(t)(1 - \eta_{\text{char},i}(t)) - P_{\text{dis},i}(t)/(1 - \eta_{\text{dis},i}(t)) - P_{\text{self, dis},i}(t) \quad (25)$$

where  $P_{\text{char},i}(t)$ ,  $P_{\text{dis},i}(t)$ ,  $P_{\text{self, dis},i}(t)$  are the charging power, discharging power and self-discharging power of energy storage, respectively;  $Q_{\text{ES},i,\min}$  and  $Q_{\text{ES},i,\max}$  are the upper and lower limits of energy storage capacity;  $\eta_{\text{dis},i}(t)$  and  $\eta_{\text{char},i}(t)$  are the discharge and charge loss rate.

### 4) Constraint of Tie-line Power with the External Grid

If the microgrid cannot meet the load demand through self-regulation, it can interact with other neighboring, non-neighboring microgrids or public grids for tie-line power. The constraints of tie line power are as follows:

$$P_{\text{neib},i,\min}^{\text{buy}} \leq P_{\text{neib},i}^{\text{buy}}(t) \leq P_{\text{neib},i,\max}^{\text{buy}} \quad (26)$$

$$P_{\text{neib},i,\min}^{\text{sell}}(t) \leq P_{\text{neib},i}^{\text{sell}}(t) \leq P_{\text{neib},i,\max}^{\text{sell}} \quad (27)$$

$$P_{\text{non\_neib},i,\min}^{\text{buy}} \leq P_{\text{non\_neib},i}^{\text{buy}}(t) \leq P_{\text{non\_neib},i,\max}^{\text{buy}} \quad (28)$$

$$P_{\text{non\_neib},i,\min}^{\text{sell}} \leq P_{\text{non\_neib},i}^{\text{sell}}(t) \leq P_{\text{non\_neib},i,\max}^{\text{sell}} \quad (29)$$

$$P_{\text{public},i,\min}^{\text{buy}} \leq P_{\text{public},i}^{\text{buy}}(t) \leq P_{\text{public},i,\max}^{\text{buy}} \quad (30)$$

$$P_{\text{public},i,\min}^{\text{sell}}(t) \leq P_{\text{public},i}^{\text{sell}}(t) \leq P_{\text{public},i,\max}^{\text{sell}} \quad (31)$$

where  $P_{\text{neib},i}^{\text{buy}}(t)$ ,  $P_{\text{neib},i}^{\text{sell}}(t)$ ,  $P_{\text{non\_neib},i}^{\text{buy}}(t)$ ,  $P_{\text{non\_neib},i}^{\text{sell}}(t)$ ,  $P_{\text{public},i}^{\text{buy}}(t)$ ,  $P_{\text{public},i}^{\text{sell}}(t)$  are the tie-line power interaction between the microgrid and neighboring microgrids, non-neighboring microgrids, and the public grid at time  $t$ .

### 5) Supply and Demand Balance Constraints

In the microgrid, distributed power generation, energy storage discharge, and power purchase from neighbors and non-neighborhoods, and external grids should be kept in line with load demand, energy storage charging, and power sold from neighbors and non-neighborhoods, and external grids.

$$P_{\text{sup}}(t) = P_{\text{dem}}(t) \quad (32)$$

where

$$P_{\text{sup}} = \sum_{i=1}^N P_{\text{MT},i}^{\text{actual}}(t) + \sum_{i=1}^M P_{\text{wind},i}^{\text{actual}}(t) + \sum_{i=1}^S P_{\text{pv},i}^{\text{actual}}(t) + \sum_{i=1}^L P_{\text{dis},i}(t) + \sum_{i=1}^p P_{\text{neib},i}^{\text{buy}}(t) + \sum_{i=1}^q P_{\text{non\_neib},i}^{\text{buy}}(t) + P_{\text{public},i}^{\text{buy}}(t) \quad (33)$$

$$P_{\text{dem}} = \sum_{i=1}^n P_{\text{crit},i}(t) + \sum_{i=1}^m P_{\text{flex},i}(t) + \sum_{i=1}^L P_{\text{char},i}(t) + \sum_{i=1}^m P_{\text{nei},i}^{\text{sell}}(t) + \sum_{i=1}^q P_{\text{non\_neib},i}^{\text{sell}}(t) + P_{\text{public},i}^{\text{sell}}(t) \quad (34)$$

## C. Model-solving Method

In this paper, the Lagrangian multiplier method and co-evolution algorithm are combined to solve the model. The former transforms the constrained optimization problem into an unconstrained optimization problem, while the latter solves the transformed unconstrained optimization problem.

The Lagrange multiplier method to solve the constrained optimization problem is expressed as follows [23]–[25]:

$$\min f(x_1, x_2, x_3, \dots, x_n) \quad (35)$$

$$\text{s.t.} \begin{cases} p_i(x_1, x_2, x_3, \dots, x_n) \leq 0 & i = 1, 2, \dots, \alpha \\ q_j(x_1, x_2, x_3, \dots, x_n) = 0 & j = 1, 2, \dots, \beta \end{cases} \quad (36)$$

where  $x = (x_1, x_2, x_3, \dots, x_n)$  are the decision variables to be optimized;  $f(x)$  represents the objective function;  $p_i(x) \leq 0$ ,

$q_j(x) = 0$  represent the  $i$ -th inequality constraint and the  $j$ -th equality constraint, respectively.

The Lagrange multiplier method transforms the constrained optimization problem into an unconstrained problem by introducing a utility function, and continuously updates the utility function in the optimization iteration, so as to obtain the optimal solution of the problem.

$$L(u, v, \omega) = f(x) + \frac{1}{2\omega} \sum_{i=1}^I \left( \left[ \max(0, u_i + \omega p_i(x)) \right]^2 - u_i^2 \right) + \sum_{j=1}^I v_j h_j(x) + \frac{\omega}{2} \sum_{j=1}^I q_j^2(x) \quad (37)$$

The correction formula of the multiplier is:

$$v_{j,k+1} = v_{j,k} + \omega q_j(x_1, x_2, \dots, x_n)_k, j = 1, 2, \dots, I \quad (38)$$

$$u_{i,k+1} = \max \left[ 0, u_{i,k} + \omega p_i(x_1, x_2, \dots, x_n)_k \right], \quad i = 1, 2, \dots, m \quad (39)$$

The judgment function is:

$$\psi_k = \sqrt{\left\{ \sum_{j=1}^I q_{j,k}^2(x) + \sum_{i=1}^m \max \left[ -p_{i,k}(x), \frac{u_{i,k}}{\omega} \right] \right\}} \quad (40)$$

When  $\psi_k = \psi(x_k) < \varepsilon$ , the iteration ends.

Next, the self-adaptive differential evolution algorithm is used to solve the unconstrained optimization problem, which is expressed as follows:

1) *Mutation*: The parent individual  $X_i^G$  performs the mutation operation to produce the mutated individual  $V_i^G$ .

$$V_i^G = X_{r1}^G + F \cdot (X_{r2}^G - X_{r3}^G) \quad (41)$$

$$V_i^G = X_{\text{best}}^G + F \cdot (X_{r1}^G - X_{r2}^G) \quad (42)$$

where  $G$  is the evolutionary generations;  $X_{r1}^G, X_{r2}^G, X_{r3}^G$  are random individuals;  $X_{\text{best}}^G$  is the optimal individual, and the variation factor is  $F \in (0, 1)$ .

2) *Crossover*: The parent individual  $X_i^G$  and the mutant individual  $V_i^G$  perform crossover operations to produce the experimental individual  $U_i^G$ .

$$U_{i,j}^G = \begin{cases} V_{i,j}^G & \text{if } \text{rand}_{i,j}(0, 1) \leq \kappa \text{ or } j = j_{\text{rand}} \\ X_{i,j}^G & \text{otherwise} \end{cases} \quad (43)$$

where the subscript  $j$  represents the  $j^{\text{th}}$  dimension of the individual  $U_i^G$ , and cross factor  $\kappa \in (0, 1)$ .

3) *Selection*:

The parent individual  $X_i^G$  and the experimental individual  $U_i^G$  compete for survival by comparing the fitness value to produce the offspring individual  $X_i^{G+1}$ .

$$X_i^{G+1} = \begin{cases} U_i^G & \text{if } f(U_i^G) \leq f(X_i^G) \\ X_i^G & \text{otherwise} \end{cases} \quad (44)$$

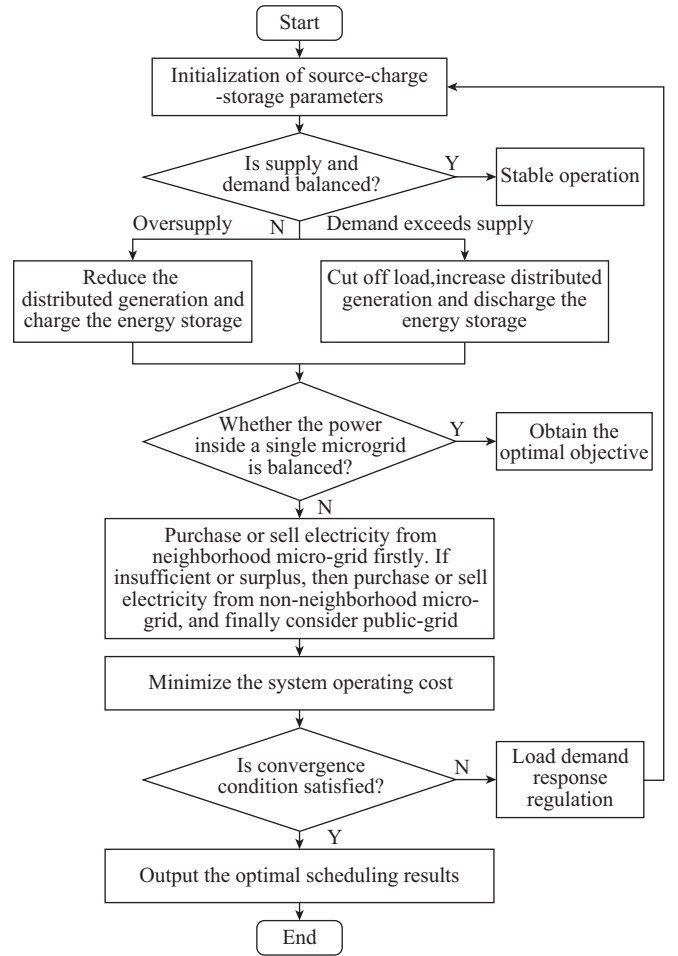


Fig. 2. Optimal scheduling method.

#### D. Energy Trading Strategy

The energy trading strategy of the microgrid is shown in Fig. 2. Regardless of whether it is buying or selling electricity, the order of microgrid transactions is to first meet its internal needs, then its neighborhood, non-neighbor microgrid, and finally the public grid.

When self-balancing cannot be achieved through self-coordination, the microgrid with low capacity will give priority to buying electricity from their neighboring microgrid, and the price of electricity is slightly higher than the transaction electricity price of the microgrid inside, but lower than buying from their non-neighboring microgrid and public grid. In contrast, the microgrid with sufficient capacity will give priority to selling electricity to their neighboring microgrid and the selling price is slightly lower than the transaction electricity price of the microgrid inside, but higher than the price of selling electricity to their non-neighboring microgrid and public grid.

## IV. CASE STUDY

### A. Parameter Settings

The configuration parameters for each component of the microgrid selected for this article are shown in Tables I–III and Fig. 3.

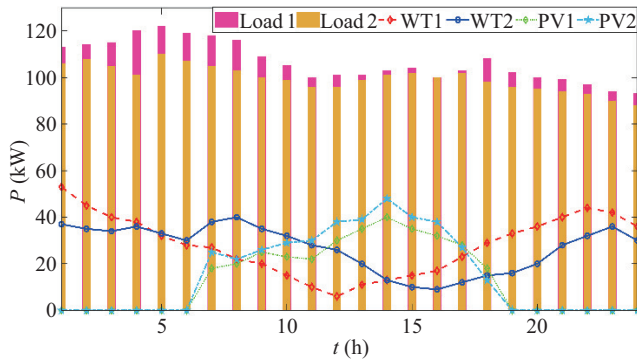


Fig. 3. Distributed generation and critical load demand/kW.

TABLE I  
DISTRIBUTED ENERGY PARAMETERS

Types	NG1	NG2	NG3	WT1	WT2	PV1	PV2
Rated/kW	210	215	220	120	130	95	100

TABLE II  
ENERGY-STORAGE PARAMETERS

Initial/kW	Rated/kW	Max/kW	Efficiency/%	Self-discharge/kWh
45	105	60	97.3	0.005

TABLE III  
NETWORKS PARAMETERS

Types	Buy/sell rates	Interaction/kW
Adjacent	1.1/0.86	[-60, 60]
Non-adjacent	1.2/0.8	[-60, 60]
Public grid	1.3/0.75	Unlimited

### B. Test Scheme Design

Depending on whether a demand response and direct connection with the same-level microgrid are considered, three typical application-schemes are established. In addition, time-sharing/real-time electricity prices (Fig. 4) are used to compare and analyze the optimization results with different schemes, which makes it possible to verify the reliability and validity of the method proposed in this paper. All tests are for 24 hours, each of which is a 1 hour increment.

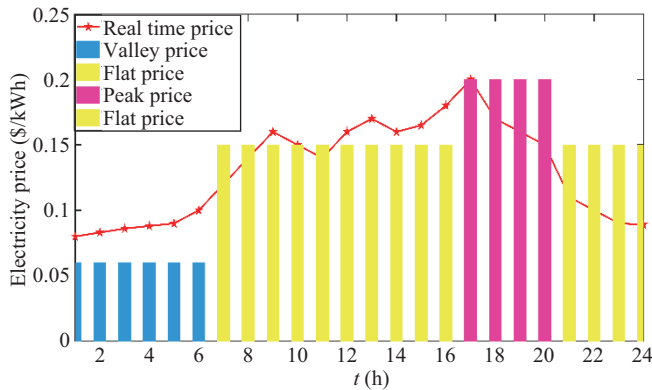


Fig. 4. Time-of-use price and real-time price during the demand response mode.

*Scheme 1:* Source-load-public grid direct-connection mode, considering the order of energy interaction within and outside the microgrid. Directly exchanged energy with the public

grid occurs as needed. This means giving priority to satisfy the supply/demand needs of the grid, while any excess or insufficient parts are directly connected. As a result, the energy exchange with the public grid is satisfactory.

*Scheme 2:* Direct-connection mode with neighboring/non-neighboring microgrids at the same level. The redundant or insufficient demand of the microgrid will interact with its neighboring and non-neighboring microgrids. If there is still a supply-demand gap after the interaction, suitable interaction/exchange with the public grid occurs.

*Scheme 3:* Demand-response mode. Based on Scheme 2, the demand-response mechanism is introduced into the energy-interaction process of the network. By adjusting the energy production for each controllable production-unit in the network, the charge/discharge status, power, and the interruption ratio of the interruptible load are enabled.

### C. Comparison of Different Schemes in Time-of-use Price and Real-time Price Scenarios

The results for the above three schemes are shown in Figs. 5, 6, and 7, respectively, in which the positive value is the microgrid purchase power and expense from the public grid, while the microgrid sell power and profit are the negative values.

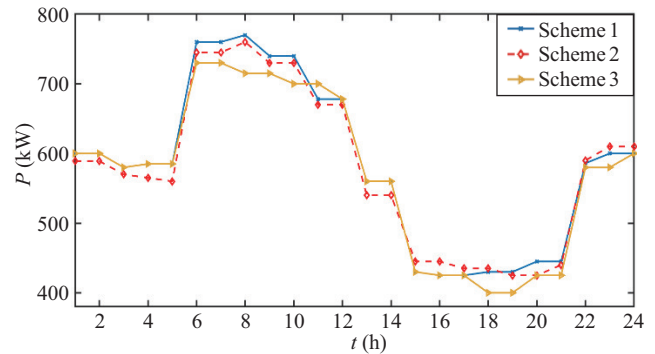


Fig. 5. Total energy consumption for the three investigated schemes.

In Fig. 5, the load demand during periods of high electricity prices is reduced to varying degrees compared with schemes 1 and 2. Because under the demand response mechanism, each energy-consuming unit is willing to interrupt part of the load in the corresponding period to obtain corresponding economic or electricity price compensation.

In Fig. 6(a) and Fig. 7(a), compared with schemes 1 and 2, the purchase of electricity from the public grid and external microgrid has different degrees of reduction, especially during periods of high electricity prices in scheme 3; In scheme 2, the microgrid purchase of electricity from the public grid is greatly reduced compared to that in scheme 1.

In Figs. 6(b) and 7(b), scheme 1 has the worst economic dispatch effect; scheme 2 has a relatively small cumulative cost value during time period  $T$  due to preferential interaction with the neighboring/non-neighborhood microgrids; In scheme 3, there is little interaction with the public grid due to the introduction of the demand response mechanism.

Table IV shows the results of the total operating costs of the microgrids during the time period  $T$ , that is, scheme 3 is

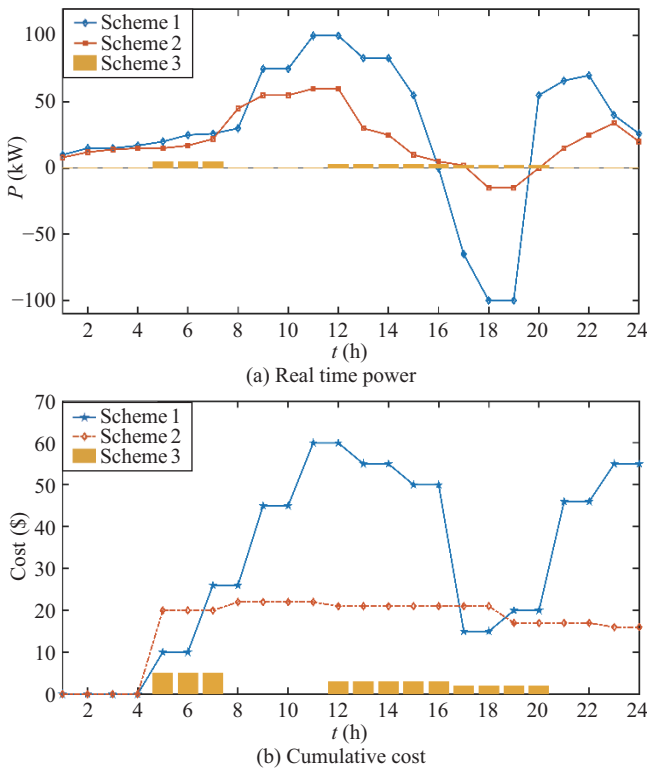


Fig. 6. Comparison of three schemes under the time-of-use price scenario.

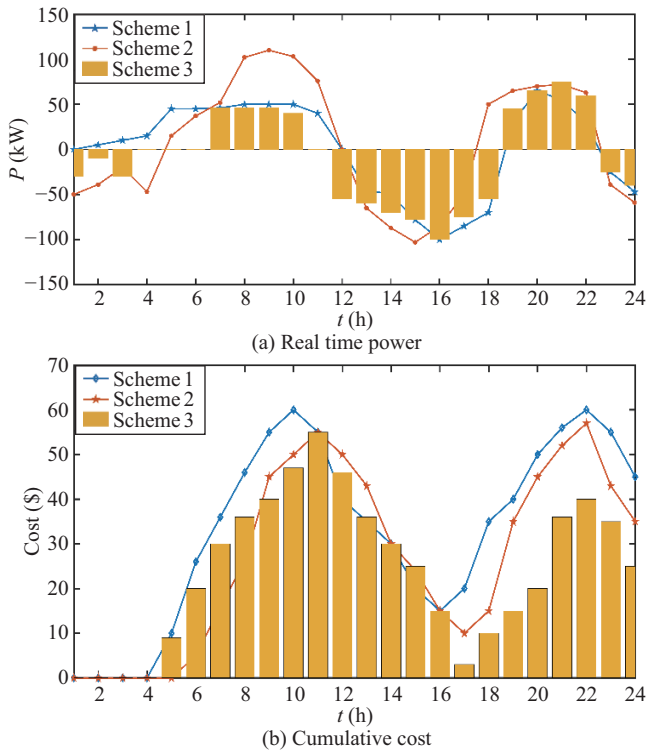


Fig. 7. Comparison of three schemes under the real time price scenario.

the best, scheme 2 is the second best, and scheme 1 is the worst.

TABLE IV  
COMPARISON OF TOTAL SYSTEM COSTS UNDER THE THREE SCHEMES

Schemes	Time-of-use price (\$)	Real-time price (\$)
Scheme I	352.57	348.6
Scheme II	335.9	330.5
Scheme III	328.6	320.7

## V. CONCLUSION

Considering full-time collaborative optimization within and outside microgrids, this paper proposes an energy management model of microgrids, and uses Lagrangian multiplier and co-evolution algorithms for a comprehensive solution. Within the network, the demand response mechanism and the economic optimization of energy storage units are introduced to realize the self-regulation, and reduce the number of power purchases from the external network. Outside the network, if the microgrid cannot achieve self-coordination, it will give priority to energy interaction with neighboring/non-neighboring microgrid and then the public grid. This method provides a new potential for further research on the hierarchical coordination of microgrids.

During 7:00–10:00 and 19:00–22:00, when the electricity price is high, in the demand response mode of scheme 3, the load consumption is reduced by about 60 kW and 30 kW compared with schemes 1 and 2, respectively. The demand response mode of scheme 3 reduces the power purchase from the public grid and external grid by about 100 kW and 50 kW compared with schemes 1 and 2, especially in the period of high electricity prices from 17:00 to 21:00. In the entire scheduling period, the total cost of the demand response mode in the time-of-use electricity price and the real-time electricity price is \$ 328.6 and \$ 320.7, respectively, which are smaller than schemes 1 and 2, and scheme 1 has the highest cost.

## REFERENCES

- [1] J. P. Yue, Z. J. Hu, C. D. Li, J. C. Vasquez, and J. M. Guerrero, "Economic power schedule and transactive energy through an intelligent centralized energy management system for a DC residential distribution system," *Energies*, vol. 10, no. 7, pp. 916, Jul. 2017.
- [2] N. Good, K. A. Ellis, and P. Mancarella, "Review and classification of barriers and enablers of demand response in the smart grid," *Renewable and Sustainable Energy Reviews*, vol. 72, pp. 57–72, May 2017.
- [3] C. Z. Shao, Y. Ding, J. H. Wang, and Y. H. Song, "Modeling and integration of flexible demand in heat and electricity integrated energy system," *IEEE Transactions on Sustainable Energy*, vol. 9, no. 1, pp. 361–370, Jan. 2018.
- [4] Q. Z. Du, W. J. Gang, S. W. Wang, J. B. Wang, and X. H. Xu, "Application of distributed energy systems in subtropical and high density urban areas," *Energy Procedia*, vol. 142, pp. 2870–2876, Dec. 2017.
- [5] I. P. Panapakidis and A. S. Dagoumas, "Day-ahead electricity price forecasting via the application of artificial neural network based models," *Applied Energy*, vol. 172, pp. 132–151, Jun. 2016.
- [6] L. Wang, Z. J. Zhang, and J. Q. Chen, "Short-term electricity price forecasting with stacked denoising autoencoders," *IEEE Transactions on Power Systems*, vol. 32, no. 4, pp. 2673–2681, Jul. 2017.
- [7] X. P. Zhang, L. Che, M. Shahidehpour, A. S. Alabdulwahab, and A. Abusorrah, "Reliability-based optimal planning of electricity and natural gas interconnections for multiple energy hubs," *IEEE Transactions on Smart Grid*, vol. 8, no. 4, pp. 1658–1667, Jul. 2017.
- [8] X. J. Zhang, G. G. Karady, and S. T. Ariaratnam, "Optimal allocation of CHP-based distributed generation on urban energy distribution networks," *IEEE Transactions on Sustainable Energy*, vol. 5, no. 1, pp. 246–253, Jan. 2014.

- [9] C. C. Shao, X. F. Wang, M. Shahidehpour, X. L. Wang, and B. Y. Wang, "Power system economic dispatch considering steady-state secure region for wind power," *IEEE Transactions on Sustainable Energy*, vol. 8, no. 1, pp. 268–278, Jan. 2017.
- [10] J. J. Zhai, X. B. Wu, S. J. Zhu, B. Yang, and H. M. Liu, "Optimization of integrated energy system considering photovoltaic uncertainty and multi-energy network," *IEEE Access*, vol. 8, pp. 141558–141568, Jul. 2020.
- [11] M. Di Somma, L. Ciabottoni, G. Comodi, and G. Graditi, "Managing plug-in electric vehicles in eco-environmental operation optimization of local multi-energy systems," *Sustainable Energy, Grids and Networks*, vol. 23, pp. 100376, Sept. 2020.
- [12] E. A. M. Ceseña and P. Mancarella, "Energy systems integration in smart districts: robust optimisation of multi-energy flows in integrated electricity, heat and gas networks," *IEEE Transactions on Smart Grid*, vol. 10, no. 1, pp. 1122–1131, Jan. 2019.
- [13] S. J. Chen, Y. B. Yang, Q. S. Xu, and J. Zhao, "Coordinated dispatch of multi-energy microgrids and distribution network with a flexible structure," *Applied Energy*, vol. 250, pp. 5553, Sept. 2019.
- [14] S. Karamdel and M. P. Moghaddam, "Robust expansion co-planning of electricity and natural gas infrastructures for multi energy-hub systems with high penetration of renewable energy sources," *IET Renewable Power Generation*, vol. 13, no. 13, pp. 2287–2297, Oct. 2019.
- [15] P. Y. Liu, T. Ding, Z. X. Zou, and Y. H. Yang, "Integrated demand response for a load serving entity in multi-energy market considering network constraints," *Applied Energy*, vol. 250, pp. 512–529, Sept. 2019.
- [16] P. P. Vergara, J. M. Rey, H. R. Shaker, J. M. Guerrero, B. N. Jørgensen, and L. C. P. Da Silva, "Distributed strategy for optimal dispatch of unbalanced three-phase islanded microgrids," *IEEE Transactions on Smart Grid*, vol. 10, no. 3, pp. 3210–3225, May 2019.
- [17] V. Sarfi and H. Livani, "An economic-reliability security-constrained optimal dispatch for microgrids," *IEEE Transactions on Power Systems*, Vol. 33, no. 6, pp. 6777–6786, Nov. 2018.
- [18] M. A. Velasquez, O. Torres-Pérez, N. Quijano, and Á. Cadena, "Hierarchical dispatch of multiple microgrids using nodal price: an approach from consensus and replicator dynamics," *Journal of Modern Power Systems and Clean Energy*, vol. 7, no. 6, pp. 1573–1584, Jun. 2019.
- [19] Y. Gao, Q. Ai, X. Wang and M. Yousif, "Distributed Cooperative Economic Optimization Strategy of a Regional Energy Network Based on Energy Cell–Tissue Architecture," *IEEE Transactions on Industrial Informatics*, vol. 15, no. 9, pp. 5182–5193, Sept. 2019.
- [20] Z. Yuan, M. R. Hesamzadeh, and D. R. Biggar, "Distribution locational marginal pricing by convexified ACOPF and hierarchical dispatch," *IEEE Transactions on Smart Grid*, vol. 9, no. 4, pp. 3133–3142, Jul. 2018.
- [21] J. S. Giraldo, J. A. Castrillon, J. C. López, M. J. Rider, and C. A. Castro, "Microgrids energy management using robust convex programming," *IEEE Transactions on Smart Grid*, vol. 10, no. 4, pp. 4520–4530, Jul. 2019.
- [22] Y. Zheng, Y. Song, D. J. Hill, and Y. X. Zhang, "Multiagent system based microgrid energy management via asynchronous consensus ADMM," *IEEE Transactions on Energy Conversion*, vol. 33, no. 2, pp. 886–888, Jun. 2018.
- [23] M. Yousif, Q. Ai, Y. Gao, W. A. Wattoo, Z. Q. Jiang, and R. Hao, "An optimal dispatch strategy for distributed microgrids using PSO," *CSEE Journal of Power and Energy Systems*, vol. 6, no. 3, pp. 724–734, Sept. 2020.
- [24] C. Q. Ju, P. Wang, L. Goel, and Y. Xu, "A two-layer energy management system for microgrids with hybrid energy storage considering degradation Costs," *IEEE Transactions on Smart Grid*, vol. 9, no. 6, pp. 6047–6057, Nov. 2018.
- [25] D. Wang, L. Liu, H. J. Jia, W. L. Wang, Y. Q. Zhi, Z. J. Meng, and B. Y. Zhou, "Review of key problems related to integrated energy distribution systems," *CSEE Journal of Power and Energy Systems*, vol. 4, no. 2, pp. 130–145, Jun. 2018.



ogy in the Energy Internet.

**Yang Gao** (S'17–M'20) received the Ph.D. degree from Shanghai Jiao Tong University, Shanghai, China, in 2019. After spending one-year post-doc research at KTH Royal Institute of Technology, Sweden, he returned to Shanghai Jiao Tong University. Currently he is an assistant professor with the Key Laboratory of Control of Power Transmission and Conversion, Shanghai Jiao Tong University, Shanghai, China. His main research interests include digital twin optimization and control of integrated energy system, microgrids, and multi-agent technology



include power quality, load modeling, smart grids, microgrid and intelligent algorithms.

**Qian Ai** (M'02–SM'15) received the bachelor's degree, master's degree and Ph.D. in Electrical Engineering from Shanghai Jiao Tong University, Wuhan University, and Tsinghua University, in 1991, 1994 and 1999, respectively. After spending one year at Nanyang Technological University, Singapore and two years at the University of Bath, UK, he returned to Shanghai Jiao Tong University. Currently he is a professor in the School of Electronic Information and Electrical Engineering, Shanghai Jiao Tong University, Shanghai, China. His main research interests